Vanadate Binding to the Gastric H,K-ATPase and Inhibition of the Enzyme's Catalytic and Transport Activities†

Larry D. Faller,*,‡ Edd Rabon,‡ and George Sachs‡

ABSTRACT: Vanadate inhibition of the catalytic and transport activities of the gastric magnesium-dependent, hydrogen ion transporting, and potassium-stimulated adenosinetriphosphatase (EC 3.6.1.3) (H,K-ATPase) has been studied. The principal experimental observations are the following: (1) Inhibition of adenosine 5′-triphosphate (ATP) hydrolysis is biphasic. Vanadate binding with a stoichiometry of 1.5 nmol mg^{-1} approximately halves K^+-stimulated ATPase activity at physiological temperature. The remaining activity is inhibited by binding an additional 1.5 nmol mg^{-1} vanadate with lower apparent affinity. (2) In the presence of both Mg^{2+} and K^+, vanadate ions bind specifically to gastric vesicles with two affinities. Vanadate binding in the presence of nucleotide is compatible with competition for the kinetically defined high-affinity and low-affinity ATP sites. (3) Vanadate inhibits phosphoenzyme formation and the K^+-stimulated *p*-nitrophenyl phosphatase activity of the enzyme monophasically. A maximum of 1.5 nmol mg^{-1} acid-stable phosphoenzyme is formed. The half-time for vanadate dissociation from the site that inhibits *p*-nitrophenyl phosphate hydrolysis is 5 min. (4) At most, 3 nmol mg^{-1} vanadate is required to inhibit proton transport. The simplest interpretation of the data is that vanadate inhibits the H,K-ATPase by binding competitively with ATP at two catalytic sites. Different catalytic mechanisms at the high-affinity and low-affinity sites are suggested by the different stoichiometries found for vanadate binding and phosphoenzyme formation.

The gastric magnesium-dependent, hydrogen ion transporting, and potassium-stimulated adenosinetriphosphatase (EC 3.6.1.3) (H,K-ATPase)[1] belongs to the class of active-transport enzymes that couple ATP hydrolysis to ion transport via the formation of an acid-precipitable phosphoenzyme intermediate. More extensively studied examples are the Na,K-ATPase and the Ca-ATPase. What is known about the structures and mechanisms of these enzymes has been compared in a recent review article (Schuurmans Stekhoven & Bonting, 1981). One similarity, in addition to the formation of a covalent phosphoenzyme intermediate, is a complex dependence of the hydrolytic rate upon ATP concentration, implying the existence of high-affinity and low-affinity catalytic and/or effector sites (or states of a single site). A vast literature is devoted to answering the following questions: How many nucleotide sites are there? How do they correlate with the number of phosphorylation sites? What is their relationship to subunit structure, and how are they expressed during the catalytic cycle?

One approach to this problem is the use of site-specific reagents. The discovery that trace amounts of vanadium in equine muscle derived ATP inhibit the Na,K-ATPase (Cantley et al., 1977) led to the use of the vanadate ion as a structural and mechanistic probe of that enzyme. Two vanadate binding sites were found per phosphorylation site, but the population of the high-affinity vanadate site inhibited greater than 95% of the ATPase activity (Cantley et al., 1978a). Subsequently, vanadate binding and high-affinity ATP binding were shown to be mutually exclusive (Smith et al., 1980). It was concluded that there is a single ATP site whose affinity for the nucleotide is reduced by the well-documented change from a high-Na^+-affinity to a high-K^+-affinity conformation of the enzyme (Jorgensen, 1975) during the catalytic cycle. Vanadate ions have been shown to slow the reversal of this conformational change (Karlish et al., 1979).

Very recently, studies of vanadate ion interactions with the Ca-ATPase were reported (Pick, 1982; Pick & Karlish, 1982). No inhibition was found of the Ca^{2+}-dependent activities of the enzyme: phosphorylation by ATP, hydrolysis of ATP, and ion transport. Micromolar concentrations of vanadate did inhibit phosphorylation by inorganic phosphate in the absence of Ca^{2+} ions, and vanadate binding was antagonized by Ca^{2+}, pyrophosphate, and high concentrations of nucleotide. The interpretation given was that a single site with different affinities for ATP in Ca^{2+} and Mg^{2+} conformers of the enzyme binds vanadate only in the low-ATP-affinity, Mg^{2+} conformation.

Although vanadate ions have been shown to inhibit the gastric H,K-ATPase (O'Neal et al., 1979), the high concentration of 10 μM required for 60% inhibition seemed to preclude the use of vanadate as a mechanistic probe. In this paper, vanadate is shown to be as potent an inhibitor of the H,K-ATPase as it is of the Na,K-enzyme. Vanadate inhibition of the catalytic and transport activities of the gastric enzyme is described and correlated with measurements of vanadate binding. The purpose of the study was to explore the number and nature of the catalytic sites. Parts of this investigation have been communicated in preliminary form (Faller et al., 1981).

† From the Laboratory of Membrane Biology, University of Alabama Medical Center, Birmingham, Alabama 35294. *Received November 15, 1982*; *revised manuscript received May 19, 1983*. This work was supported by U.S. Public Health Service Grant AM-28459 and National Research Service Award Senior Fellowship AM-06460 awarded to L.D.F.

‡ Present address: Department of Medicine, UCLA School of Medicine, and the Center for Ulcer Research and Education, Veterans Administration Wadsworth Hospital Center, Los Angeles, CA 90073.

[1] Abbreviations: H,K-ATPase, magnesium-dependent, hydrogen ion transporting, and potassium-stimulated adenosinetriphosphatase (EC 3.6.1.3); Na,K-ATPase, magnesium-dependent and sodium- and potassium-stimulated adenosinetriphosphatase; Ca-ATPase, calcium- and magnesium-dependent adenosinetriphosphatase; ATP, adenosine 5′-triphosphate; pNPP, *p*-nitrophenyl phosphate; pNPPase, *p*-nitrophenyl phosphatase; CDTA, *trans*-1,2-diaminocyclohexane-*N*,*N*,*N*′,*N*′-tetraacetic acid; Tris, tris(hydroxymethyl)aminomethane; AO, acridine orange; TNP-ATP, 2′,3′-*O*-(2,4,6-trinitrocyclohexadienylidine)-ATP.

0006-2960/83/0422-4676$01.50/0

Experimental Procedures

Materials

Gastric Vesicles. The H,K-ATPase used in most of the experiments that will be reported was isolated from hog stomachs by the discontinuous gradient method (Chang et al., 1979). The vesicles in which the enzyme is found were recovered from the 0.25 M sucrose–7% (w/w) Ficoll interface and are only slowly permeable to ions. Two hours were required to equilibrate KCl across the membrane at room temperature. Vesicles were kept intact for sidedness and transport experiments by dilution into nearly isotonic solutions. Broken vesicles, which are freely permeable to alkali metal ions, were prepared by suspension in deionized water and lyophilization. They were stored at −80 °C.

As a control for enzyme heterogeneity, vesicles from the 1.08–1.12 density band of a continuous Ficoll–sucrose gradient, that had been further purified by free-flow electrophoresis, were utilized in some experiments. These vesicles have been shown to be free of all other enzyme activities except pNPPase, and 75% or more of the protein they contain migrates electrophoretically in the the 1.0×10^5 dalton band of sodium dodecyl sulfate–polyacrylamide gels (Saccomani et al., 1977). Sample protein was determined by the Lowry method using bovine serum albumin standards (Lowry et al., 1951). The molecular weight of 3.0×10^5 found by target size analysis of vesicles purified by free-flow electrophoresis (Saccomani et al., 1981) was used to calculate the enzyme concentration.

Reagents. [γ-^{32}P]ATP and [^{48}V]$VOCl_3$ were purchased from Amersham. Vanadium-free ATP and the ditris salt of pNPP were obtained from Sigma, gold-label vanadyl sulfate and ammonium metavanadate were from Aldrich, and sodium orthovanadate was from Fisher Scientific Co. AO from Eastman was used without further purification. All other reagents were the highest grade available.

Methods

ATPase. ATP hydrolysis was measured by the method of Yoda & Hokin (1980). Details of the reaction mixtures are given in the figure legends. In addition, experiments with intact vesicles were 0.2 M in sucrose and contained 5 μg mL^{-1} nigericin. Since vanadium has been reported to equilibrate slowly with the Na,K-ATPase (Cantley et al., 1978a), the gastric enzyme and its cofactors were preincubated with the vanadium salt for 5 min at 37 °C before the reaction with ATP was initiated. Longer incubation times up to 1 h did not affect either the measured rate or the dependence of the rate upon vanadium concentration. The reaction was stopped after 15 min. The assay was shown to be linear over this time period by measuring the specific K^+-ATPase activity at 4, 8, 12, and 16 min. The result at 1.8 nM vanadate, expressed as a percentage of the uninhibited activity, was 75.8 ± 4.1%, and at 1.8 μM vanadate, the result was 26.3 ± 2.8%. There has also been some question whether the 4+ (Post et al., 1979) or 5+ (Macara et al., 1980) oxidation state of vanadium is the form that inhibits the Na,K-ATPase, so vanadyl sulfate and also the ammonium and sodium salts of meta- and orthovanadate were used in different titrations. The results obtained with all three salts were indistinguishable, consistent with rapid oxidation of vanadyl to vanadate (Dean & Herringshaw, 1963) which exists largely as the monoanion $H_2VO_4^-$ at pH 7.4 (Cotton & Wilkinson, 1974), and therefore, the data have been combined.

pNPPase. The purified gastric H,K-ATPase also catalyzes the hydrolysis of pNPP. Advantage was taken of the color change that accompanies *p*-nitrophenylate ion formation to follow the rate at which vanadate inhibits the gastric enzyme, as well as the extent of inhibition. Figure 1 illustrates a concentration-jump experiment. The pNPPase reaction was started in an Aminco DW2 dual-beam spectrophotometer set at 402 and 500 nm. The uninhibited steady-state rate was evaluated from the initial linear change in absorbance with time (R_0) and the molar absorptivity of the *p*-nitrophenylate ion at 402 nm and pH 7.4 (1.0×10^4 M^{-1} cm^{-1}). At an arbitrary time zero, a small aliquot of vanadate was added through a light-tight hole in the cell compartment cover to the reaction cuvette, which was equipped with a magnetic stirrer. The relaxation time (τ) was found by fitting the experimental absorbance vs. time curve with a nonlinear least-squares program to the equation (Cantley et al., 1978a)

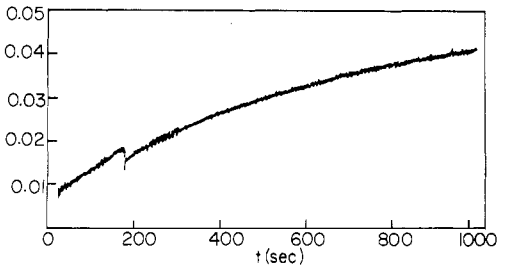

FIGURE 1: Concentration-jump experiment. The uninhibited steady-state rate of pNPP hydrolysis (R_0, initial linear change in absorbance with time) was perturbed at an arbitrary time zero (vertical deflection) by the addition of vanadate. The time (τ), in this experiment 260 s, required for relaxation to the inhibited steady-state rate (R_f, final linear change in absorbance with time) was found by fitting the curve to eq 1. Final experimental conditions: 10 μM Na_3VO_4, 6 mM pNPP, 2 mM $MgCl_2$, 10 μg mL^{-1} protein, and 40 mM Tris-HCl at pH 7.4 and 37 °C.

$$A = A_0 + R_f t + (R_0 - R_f)(1 - e^{-t/\tau}) \qquad (1)$$

in which A_0 is the absorbance at time zero and A is the absorbance at subsequent times t. The inhibited steady-state rate to which the system relaxes was evaluated from the final linear change in absorbance with time (R_f).

Phosphorylation. The steady-state amount of acid-stable phosphoenzyme formed was measured as described by Post (Post & Sen, 1967). The reaction was initiated by adding γ-^{32}P-labeled ATP and stopped after 15 s (Wallmark et al., 1980) by adding either an equal volume or a 5-fold excess of 12% trichloroacetic acid containing 6 mM inorganic phosphate and 1.5 mM cold ATP. The precipitated membrane was collected on a 3-μm Millipore filter, washed 5 times with 5- or 10-mL aliquots of 3% trichloroacetic acid containing 2 mM inorganic phosphate, dispersed in scintillation fluid, and counted. The background count was established by reversing the order in which ATP and the stop solution were added.

Vanadate Binding. ^{48}V-Labeled vanadate binding was measured by the rapid sedimentation method (Howlett et al., 1978). In competition experiments, ATP was added first and then vanadate. After the mixture was incubated with the enzyme for 5 min, 175 μL of the reaction mixture was centrifuged for 30 min at 30 psi in a Beckman airfuge, which corresponds to about 95000 rpm and 148000*g*. A 100-μL aliquot of the supernatant was counted. After the centrifuge tube was drained and dried with a cotton swab, the pellet was resuspended in 50 μL of deionized water, combined with a 100-μL 10% (w/w) sodium dodecyl sulfate wash of the centrifuge tube, and counted. Measurements at 37 °C were made by placing the centrifuge in an environmental room and passing the drive air through 50 ft of copper tubing submersed in a thermostated bath. Control experiments in which the vesicles

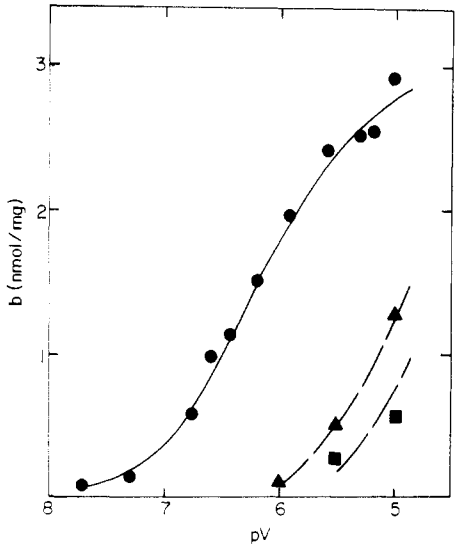

FIGURE 2: Vanadate binding to broken gastric microsomal vesicles in the absence of K^+. Bound vanadate (b) is plotted against minus the log of the free vanadate concentration (pV). (●) 2 mM $MgCl_2$. The solid line was calculated for binding to a single class of sites with a dissociation constant of 0.6 μM. (▲) 2 mM $MgCl_2$ and 2 mM ATP; (■) 0.3 mM CDTA. Other experimental conditions: 268 μg mL^{-1} protein and 40 mM Tris-HCl at pH 7.4 and 22 °C.

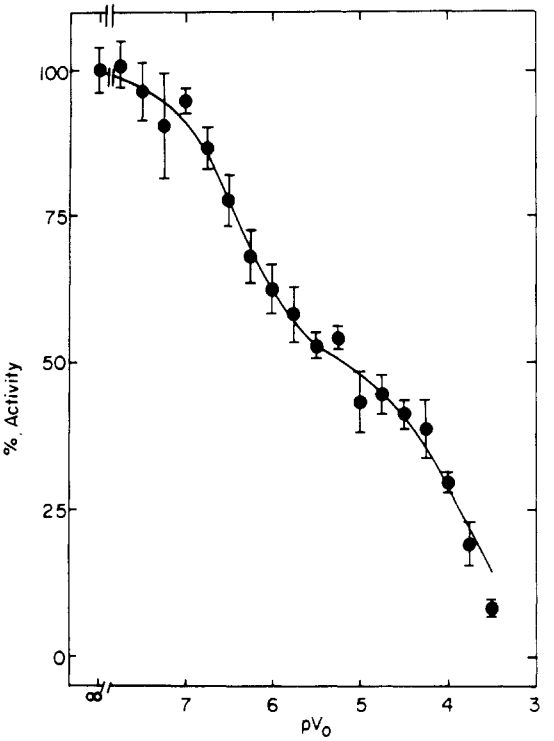

FIGURE 3: Vanadate inhibition of the Mg^{2+}-ATPase activity of broken gastric vesicles. The percentage of full activity (no vanadate) remaining at each total vanadate concentration (V_0 in the figure) is plotted. The vertical bars show the sample standard deviations in the measurements. The solid line was calculated for binding to two independent classes of sites with apparent dissociation constants of 0.3 μM and 0.1 mM, as described in the text. Experimental conditions: 2 mM ATP, 2 mM $MgCl_2$, 50 μg mL^{-1} protein, and 40 mM Tris-HCl at pH 7.4 and 37 °C.

were centrifuged for 5 or 15 min gave identical results. ATP is hydrolyzed slowly by the gastric enzyme at room temperature (Wallmark et al., 1980), but in the 37 °C experiments, the ratio of ATP to ADP did vary, depending upon the percentage of the enzyme inhibited by vanadate. This should not have affected the results markedly, because measurements of ATP and ADP binding to gastric microsomes by following displacement of the fluorescent nucleotide analogue TNP-ATP indicate that both bind with about the same affinity (unpublished results).

Proton Transport. Accumulation of the weak base AO inside intact vesicles was used to measure proton transport (Rabon et al., 1978). In one type of experiment, the ratio of vanadate to enzyme was kept constant. Vesicles preloaded with 150 mM KCl, 2 mM $MgCl_2$, and 10 mM Tris-HCl buffer at pH 7.4 were incubated with varying amounts of sodium vanadate for 5 min at 37 °C. They were then diluted into 150 mM choline chloride containing 2 mM $MgCl_2$, 10 mM Tris-HCl, and 10 μM AO to give a K^+ concentration outside of 7 mM. In another type of experiment, the concentration of vanadate was maintained constant. Following incubation with vanadate for 5 min, KCl-loaded vesicles were diluted 22-fold into a choline chloride solution which also contained vanadate. In this type of experiment, the concentration of the inhibitor was the same in the incubation and final solutions, but the ratio of vanadate to enzyme was much higher in the final solution. In both types of experiment, transport was initiated by adding ATP adjusted to pH 7.4. Changes in AO absorbance were measured with a DW2 dual-beam spectrophotometer set at 492 and 546 nm. The maximum rate of proton transport, which occurred within 3 min, was evaluated from the maximum slope of the absorbance vs. time curve.

Results

Binding to the Mg^{2+}-Enzyme. Measurements of vanadate binding to broken gastric microsomal vesicles in the absence of K^+ are shown in Figure 2 (circles). Each point is the average of duplicate determinations. Of the counts, 97 ± 6% were recovered in the experiments reported. No correction has been made for trapped counts or for nonspecific binding below 10 μM vanadate, because in these experiments and those reported later the result at any vanadate concentration was independent of the specific activity of the titrant, and saturation was apparent in the 5–10 μM concentration range. Interpretation of the small amount of binding to apoprotein (0.3 mM CDTA) observed in this concentration range (squares) as preferential binding to specific sites gives an estimate of 50-fold for the enhancement of vanadate affinity by the divalent cation. The shape of the titration curve obtained in the presence of Mg^{2+} indicates binding to a single class of sites. The solid line in Figure 2 was calculated for a vanadate dissociation constant (K_d) of 0.6 μM and an average binding stoichiometry of 3 nmol mg^{-1}. Measurements at 37 °C gave an average saturation value of 3.1 nmol of vanadate bound per mg of protein. ATP competes with vanadate (triangles). An apparent dissociation constant of 13 μM can be estimated from the limited amount of vanadate binding seen below 10 μM ligand in the presence of both ATP and Mg^{2+}.

Inihibition of Mg^{2+}-ATPase Activity. In contrast to vanadate binding, inhibition of the Mg^{2+}-ATPase activity of broken gastric vesicles was biphasic. The mean of from four to eight activity measurements and the sample standard deviation at each vanadate concentration are plotted in Figure 3. The rate measured in the absence of vanadium was 6.3 ± 1.3 μmol mg^{-1} h^{-1}. The solid line was drawn by assuming two classes of independent vanadate binding sites:

(2)

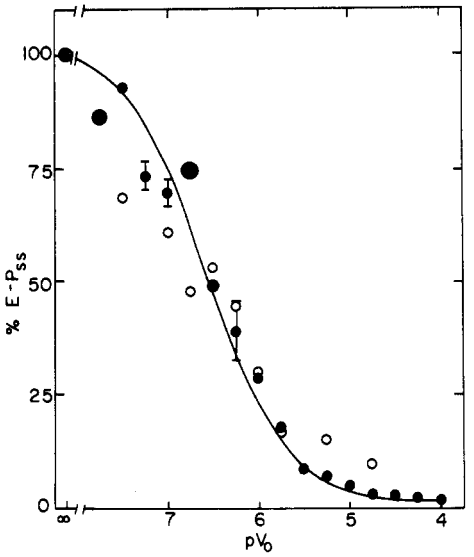

FIGURE 4: Vanadate inhibition of the steady-state level of phosphoenzyme formed by broken gastric vesicles. % E–P_{ss} is the steady-state phosphoenzyme level formed at each vanadate concentration, expressed as a percentage of the steady-state phosphoenzyme level formed in the absence of vanadate. The scatter in the measurements is indicated either by the size of the circles or by the length of the vertical bars. The solid line was calculated for a single class of inhibitory sites with an apparent inhibition constant of 0.2 μM. (●) 2 μM [γ-^{32}P]ATP at 22 °C; (○) 0.2 mM [γ-^{32}P]ATP at 37 °C. Other conditions: 2 mM $MgCl_2$, 50 μg mL^{-1} protein, and 40 mM Tris-HCl at pH 7.4.

The concentration of free vanadate ([V]) can then be found by solving the cubic equation (Uspensky, 1948)

$$[V]^3 + (K_1 + K_2 + 2[E]_0 - [V]_0)[V]^2 + [K_1K_2 + (K_1 + K_2)([E]_0 - [V]_0)][V] - K_1K_2[V]_0 = 0 \quad (3)$$

and the percent activity predicted from the expression

$$\% \text{ activity} = 100\left[\left(\frac{K_1}{K_1 + [V]}\right)X_1 + \left(\frac{K_2}{K_2 + [V]}\right)X_2\right] \quad (4)$$

in which K_i and X_i are the apparent inhibition constant and the fractional activity associated with the ith class of sites, respectively. The values used to obtain the fit shown were K_1 = 0.3 μM, X_1 = 0.5, K_2 = 0.1 mM, and X_2 = 0.5.

Inhibition of Phosphorylation. Since vanadium in the 5+ oxidation state can assume the trigonal-bipyramidal geometry of pentacoordinate phosphorus (Van Etten et al., 1975; Lopez et al., 1976), vanadate is thought to inhibit phosphohydrolases that react via a phosphoenzyme intermediate by acting as a transition-state analogue. The results in Figure 4 show that vanadate does inhibit the gastric H,K-ATPase at the phosphorylation step of the reaction. Inhibition was monophasic, and the apparent inhibition constant was the same at 2 and 200 μM ATP. The solid line was calculated for a single class of vanadate binding sites with an apparent inhibition, or binding, constant of 0.2 μM.

Table I summarizes previously published and newly measured values of the steady-state amount of phosphoenzyme (E–P_{ss}) formed in the Mg^{2+}-ATPase reaction. In the absence of K^+, the phosphorylation rate of the gastric enzyme has been shown to be more than 2 orders of magnitude faster than the dephosphorylation rate (Wallmark & Mardh, 1979; Wallmark et al., 1980), so phosphorylation is presumably complete in the steady state. Yet the maximum steady-state phosphoenzyme level that has been reported (1.5 nmol mg^{-1}) is only half the stoichiometry found for vanadate binding to the

Table I: Stoichiometry of Steady-State Phosphoenzyme Formation[a]

[ATP] (μM)	E–P_{ss} (nmol mg^{-1})	±σ	n	ref
5100	1.5	10%		Wallmark & Mardh (1979)
1-200	1.1-1.5			Wallmark et al. (1980)
1	1.28	0.10	3	this study
2	1.21	0.22	3	
5	1.35	0.27	6	
10	1.41	0.19	4	
20	1.28	0.19	6	
50	1.49	0.23	4	
100	1.52	0.38	4	
200	1.72	0.59	4	
400	1.35	0.09	3	
500	1.80	0.36	6	
750	1.39	0.48	4	
5-750	1.48	0.31	41	

[a] Experimental conditions: 2 mM $MgCl_2$, 50 μg mL^{-1} protein, and 40 mM Tris-HCl at pH 7.4 and 22 or 37 °C.

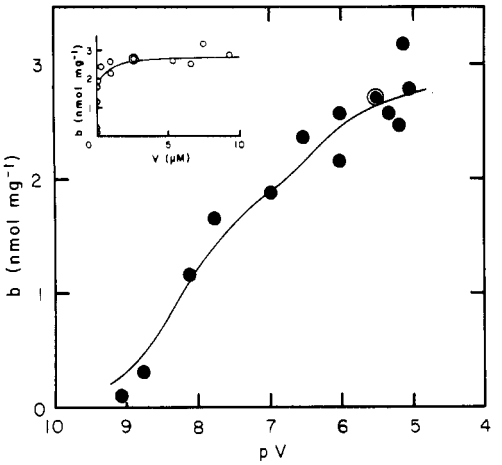

FIGURE 5: Vanadate binding to gastric vesicles in the presence of K^+ and Mg^{2+} at 22 °C. Saturation occurred when 2.8 ± 0.3 nmol mg^{-1} vanadate was bound (inset). The solid lines were calculated for binding to two independent sites with dissociation constants (K_d) of 5 nM and 0.5 μM and stoichiometries of 1.8 nmol mg^{-1} at the high-affinity site and 1 nmol mg^{-1} at the lower affinity site. Other experimental conditions: 2 mM $MgCl_2$, 7 mM KCl, 265 μg mL^{-1} protein, and 40 mM Tris-HCl at pH 7.4.

Mg^{2+}-enzyme (3 nmol mg^{-1}). One possible explanation is that phosphorylation of the lower affinity (K_{m_2} = 50 μM) of the kinetically defined ATP sites (Wallmark et al., 1980) was missed, because most of the published measurements of phosphorylation were made at low ATP concentrations where only the higher affinity (K_{m_1} = 0.4 μM) of the kinetically defined ATP sites would be active. Therefore, the reaction was reinvestigated in the range of ATP concentrations from 5 to 750 μM. The results confirm that phosphorylation is maximal when the ATP concentration is just high enough to saturate the high-affinity ATP site (5 μM) and that the maximum acid-stable phosphoenzyme level (1.5 ± 0.3 nmol mg^{-1}) is half the vanadate binding stoichiometry. With the caution that the standard error increases because of the greater technical difficulty of phosphorylation measurements at higher ATP concentrations, there is no evidence in Table I for phosphorylation of a low-affinity ATP site in the substrate concentration range where the overall hydrolytic reaction rate more than doubles (Wallmark et al., 1980).

Binding to the K^+-Enzyme. Vanadate binding to gastric microsomal vesicles in the presence of both K^+ and Mg^{2+} was

Table II: Comparison of Substrate Constants Predicted from Vanadate Binding Data with Michaelis Constants Reported in the Literature

temp (°C)	site	predicted[a] K_s (μM)	reported[b] K_m (μM)	ref
37[c]	high affinity	69[d]	17	Schrijen (1981)[e]
			74	Sachs et al. (1980)[f]
	low affinity	860[g]	470	Schrijen (1981)
			1100	Sachs et al. (1980)
22	high affinity	20[h]	3.5	Wallmark et al. (1980)[i]
	low affinity	400[j]	30	Wallmark et al. (1980)

[a] $K_s = K_d[ATP]_0/[K_d(app) - K_d]$; 2 mM ATP, 7 mM KCl, and 40 mM Tris-HCl, pH 7.4. [b] Evaluated from curved Eadie–Hofstee plots. Free $[Mg^{2+}]$ varied. [c] ATP/ADP ratio varied. [d] K_d = 20 nM, K_d(app) = 0.6 μM (Figure 7). [e] 2 mM $MgCl_2$, 20 mM KCl, 6.25–2000 μM ATP, and 30 mM imidazole hydrochloride, pH 7.0. [f] 2 mM $MgCl_2$, 20 mM KCl, 2.5–2000 μM ATP, and 40 mM Tris-HCl, pH 7.4. [g] K_d = 0.6 μM, K_d(app) = 2 μM (Figure 7). [h] K_d = 5 nM (Figure 5), K_d(app) = 0.5 μM (Figure 6). [i] 2 mM $MgCl_2$, 2.5 mM KCl, 0.1–2000 μM ATP, and 40 mM Tris-HCl, pH 7.4. [j] K_d = 0.5 μM (Figure 5), K_d(app) = 3 μM (Figure 6).

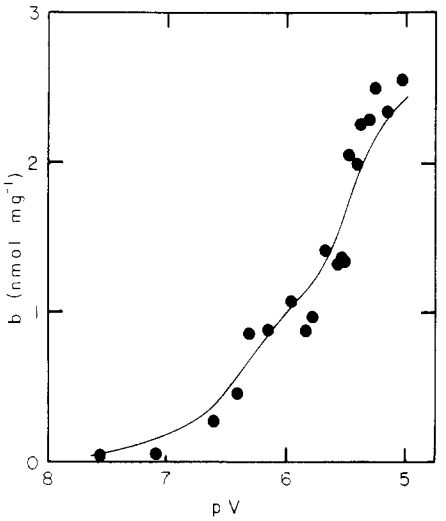

FIGURE 6: Vanadate binding to gastric vesicles in the presence of 2 mM ATP at 22 °C. The solid line was drawn for binding to two independent sites with apparent dissociation constants [K_d(app)] of 0.5 and 3 μM. Other experimental conditions were the same as those given for Figure 5.

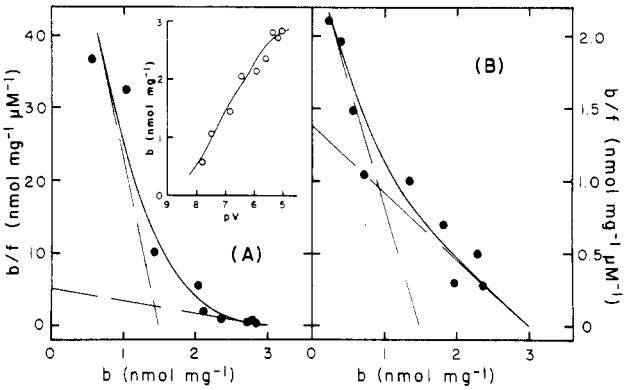

FIGURE 7: Vanadate binding to gastric vesicles in the presence of K^+ and Mg^{2+} at 37 °C. Scatchard plots of the ratio of bound (b) to free vanadate (f) against the amount bound (A) in the absence and (B) in the presence of 2 mM ATP. Each point is the average of two measurements. The dissociation constants (K_d) of 20 nM and 0.6 μM given by the slopes of the asymptotes drawn to the curve in (A) were used to calculate the solid line for binding to two independent sites in the semilogarithmic plot in the inset. The apparent dissociation constants [K_d(app)] evaluated from the asymptotes to the curve drawn in (B) were 0.6 and 2 μM. Other conditions: 2 mM $MgCl_2$, 7 mM KCl, 241 μg mL^{-1} protein, and 40 mM Tris-HCl at pH 7.4.

measured at room temperature and at 37 °C. The 22 °C data are shown in Figure 5. Of the counts, 93 ± 8% were recovered. It can be seen from the plot of the measured values of bound vanadate against the measured concentration of free vanadate in the inset that saturation occurred with the same stoichiometry (2.8 ± 0.3 nmol mg^{-1}) found for vanadate binding to the Mg^{2+}-enzyme. However, the ratio of the free vanadate concentrations that corresponded to 90% bound and 10% bound was over 1000 in the case of the K^+-enzyme, compared to the value of 81 expected for binding to a single class of sites and found for vanadate binding to the Mg^{2+}-enzyme. This can be seen clearly when the same date are plotted in semilogarithmic form. Evidently, in the presence of K^+, there are two classes of vanadate binding sites. The solid line in Figure 5 was calculated by assuming a dissociation constant for 64% of the vanadate of 5 nM and a dissociation constant for the remaining vanadate of 0.5 μM. Figure 6 is a semilogarithmic plot of vanadate bound to the K^+-enzyme in the presence of 2 mM ATP at 22 °C vs. the concentration of vanadate that remained free. In this case, the data can be fitted about equally well by assuming either a single site or two sites with numerically similar apparent affinities for vanadate. The reasons for preferring the latter interpretation are explained under Discussion. The solid line in Figure 6 demonstrates that the data can be fitted by assuming two apparent dissociation constants of 0.5 and 3 μM. The substrate dissociation constants that would be needed to explain the weaker binding of vanadate observed in the presence of ATP by competition between the ligands have been calculated and are recorded in column 3 of Table II.

The 37 °C binding data are summarized in Figure 7. In the absence of nucleotide, the ratio of the free vanadate concentrations that correspond to 90% bound and 10% bound was about 500, compared to the theoretical value of 81 for binding to a single class of sites. This is easiest to see in the semilogarithmic plot of the data shown in the inset to Figure 7A. An alternative way of graphically demonstrating binding heterogeneity is the curvature of a plot of bound ligand over free vs. bound ligand. Figure 7A is a Scatchard plot of the same data for vanadate binding to gastric microsomes at 37° C. Each plotted point is the average of two measurements. The dissociation constants calculated from the slopes of the asymptotes shown drawn to the curve were 20 nM and 0.6 μM. The solid line in the inset was calculated for binding to two sites with equal stoichiometries and dissociation constants inferred from the Scatchard plot. Figure 7B is a Scatchard plot of the results obtained in the presence of nucleotide. In this case, the data are compatible with vanadate binding either to a single site or to two sites with numerically similar apparent vanadate dissociation constants. If two sites are supposed, consistent with the evidence in Figure 7A for two sites in the absence of nucleotide, apparent dissociation constants of 0.6 and 2 μM can be roughly estimated from the asymptotes shown drawn to the curve in Figure 7B. The nucleotide dissociation constants predicted by assuming competitive binding with vanadate are recorded in Table II.

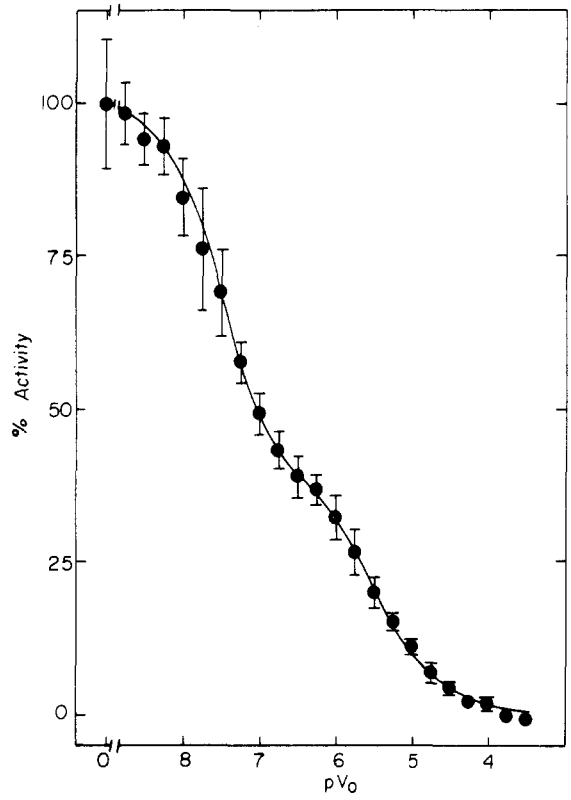

FIGURE 8: Vanadate inhibition of the K^+-ATPase activity of broken gastric vesicles. The vertical bars show the sample standard deviations in the measurements. The solid line was calculated as described in the text for two classes of independent inhibitory sites with apparent dissociation constants of 12 nM and 3 μM. Experimental conditions: 2 mM ATP, 2 mM $MgCl_2$, 7 mM KCl, 10 μg mL^{-1} protein, and 40 mM Tris-HCl at pH 7.4 and 37 °C.

Inhibition of K^+-ATPase Activity. The K^+-stimulated ATPase activity of broken gastric vesicles was measured as a function of vanadate ion concentration at physiological temperature. The results from six independent titrations, in which four different vesicle preparations were used, are summarized in Figure 8. The rate measured in the absence of vanadium was 142 ± 15 μmol mg^{-1} h^{-1}. The points are the mean of from 8 to 22 measurements at each inhibitor concentration, and the vertical bars show the sample standard deviations. The titration curve was unchanged by shortening the assay to 8.5 min. Experimentally indistinguishable results were obtained by titrating vesicles that had been further purified by free-flow electrophoresis. A titration of intact vesicles showed the same biphasic inhibition pattern.

Vanadate inhibition of K^+-ATPase activity closely parallels vanadate inhibition of Mg^{2+}-ATPase activity, strengthening the conclusion drawn from antibody cross-reactivities (Saccomani et al., 1979) and steady-state phosphoenzyme measurements (Wallmark et al., 1980) that the two activities are alternative reaction pathways of the same enzyme. The solid line in Figure 8 was drawn by using eq 3 and 4 for two classes of independent binding sites with K_1 = 12 nM, X_1 = 0.6, K_2 = 3 μM, and X_2 = 0.4. Since approximately halving the assay time gave experimental points that fell on the same curve, the observed titration cannot be an artifact of the method used to measure ATPase activity. In the presence of K^+, vanadate appears to bind about 30 times tighter to both sites. Both the activity inhibitable by high-affinity vanadate and the activity inhibitable by low-affinity vanadate are stimulated about 20-fold by K^+, so neither activity can be due to mitochondrial contamination. The explanation cannot be that there are internal and external sites for vanadate, because intact vesicles

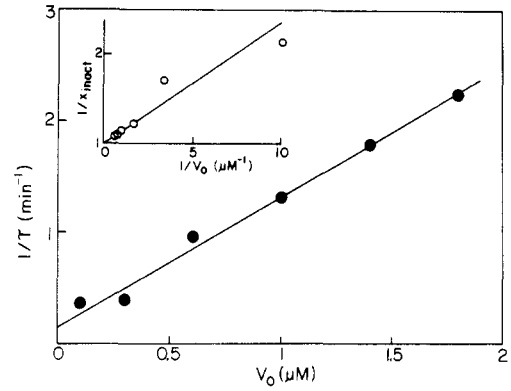

FIGURE 9: Rate of vanadate interaction with the K^+-enzyme. The reciprocal relaxation times measured in concentration-jump experiments, as illustrated in Figure 1, are plotted against the total vanadate concentration used to perturb the uninhibited steady state. The ordinate intercept gives the reverse rate constant, the slope the forward rate constant, and their quotient the vanadate dissociation constant. The half-time for vanadate dissociation from the site that inhibits pNPPase activity is 4.6 min. The inset is a double-reciprocal plot of the fraction inactive (X_{inact}), evaluated from the final and initial slopes of the relaxation curves ($1 - R_f/R_0$), vs. the total vanadate concentration. The apparent vanadate-inhibition constant was found from its slope. Assay conditions: 6 mM pNPP, 2 mM $MgCl_2$, 7 mM KCl, 10 μg mL^{-1} protein, and 40 mM Tris-HCl at pH 7.4 and 38 ± 1 °C.

were also inhibited biphasically. The reproducibility of the vanadate inhibition pattern obtained with different step-gradient preparations, as well as with electrophoretically purified vesicles, makes it unlikely that gastric vesicles contain two ATPases. If two different enzymes were present, not only would they have to copurify and be stimulated by K^+ to the same extent but also they would both have to be composed of 1.0×10^5 dalton polypeptides (Saccomani et al., 1977) and have the same functional molecular weight (Saccomani et al., 1981).

Inhibition of pNPPase Activity. In Figure 9, the reciprocal of the relaxation time measured for inhibition of K^+-stimulated pNPPase activity is plotted vs. the vanadate added in concentration-jump experiments. For bimolecular association of inhibitor with enzyme

$$E + V \underset{k_{-1}}{\overset{k_1}{\rightleftharpoons}} EV \tag{5}$$

linearity is predicted

$$1/\tau = k_1[V]_0 + k_{-1} \tag{6}$$

provided $[V]_0 > [E]_0$. The slope of the straight line shown drawn through the experimental points gives a forward rate constant of 1.2×10^6 M^{-1} min^{-1} and the ordinate intercept a reverse rate constant of 0.15 min^{-1}. The half-time for vanadate dissociation from the K^+-enzyme is therefore 4.6 min. The quotient of the reverse and forward rate constants gives a dissociation constant for vanadate of 125 nM under these experimental conditions. It is in good numerical agreement with the apparent dissociation constant of 135 nM evaluated from the inhibited steady-state rates. The fraction of the enzyme complexed with vanadate was assumed to be inactive:

$$X_{inact} = \frac{[EV]}{[E]_0} = \frac{[V]_0}{[V]_0 + K_d(app)} \tag{7}$$

and the apparent dissociation constant was found from the slope of the double-reciprocal plot shown in the inset to Figure 9. The uninhibited rate was 58 μmol mg^{-1} h^{-1}. In the absence of K^+, the uninhibited rate was only 2.5 μmol mg^{-1} h^{-1}, precluding accurate measurements of the variation in the relax-

Table III: Vanadate Inhibition of Proton Transport by Gastric Microsomal Vesicles[a]

preincubation[b]		constant ratio ($V_f/P_f = V_i/P_i$)		constant concn ($V_f = V_i$)	
V_i (μM)	V_i/P_i (nmol mg^{-1})	V_f (nM)	R_{max} (%)	V_f/P_f (nmol mg^{-1})	R_{max} (%)
0	0	0	100	0	100
0.11	0.17	5	91	3.6	80
0.22	0.34			8.7	53
0.42	0.68			14.4	49
0.64	1.02	30	57	24	18
0.85	1.36			29	14
1.06	1.70	50	26	40	12
1.51	2.40	70	18	61	7
1.94	3.25	100	8	79	6
2.38	3.79			96	5

[a] Initial experimental conditions: 150 mM KCl inside, 7 mM KCl outside, 2 mM ATP, 2 mM $MgCl_2$, 26.8 μg mL^{-1} protein, 10 μM AO, and 10 mM Tris-HCl at pH 7.4 and 37 °C. [b] Preincubation conditions: 150 mM KCl, 2 mM $MgCl_2$, 0.58 mg mL^{-1} protein, and 10 mM Tris-HCl at pH 7.4 and 37 °C.

ation time with vanadate concentration. However, it is apparent from the experiment shown in Figure 1 that vanadate also interacts slowly with the Mg^{2+}-enzyme.

Inhibition of Proton Transport. The effect of vanadate ions on the rate of proton transport by intact gastric vesicles is summarized in Table III. The maximum transport rate is expressed as a percentage of the uninhibited rate, so that the results obtained with two different vesicle preparations could be combined. Each tabulated value is the average of from two to five measurements with an average standard deviation of 11%. The vanadate concentrations with which the vesicles were preincubated are given in the first two columns. Dilution of the vesicles into additional vanadate (columns 5 and 6) always resulted in greater inhibition than dilution into vanadate-free medium (columns 3 and 4). However, at the same final concentration of vanadate, much less inhibition was observed in the constant concentration experiments. For example, the transport rate was 92% inhibited in the constant vanadate to protein ratio experiment but only 20% inhibited in the constant concentration experiment when the final vanadate concentration was 0.1 μM. This suggests that equilibrium was not reached in these experiments, presumably because of the slow rate at which vanadate interacts with gastric microsomes. Preincubation with 3 nmol mg^{-1} vanadate was enough to inhibit the transport rate more than 90%. Complete inhibition after preincubation for 5 min with intact vesicles indicates that vanadate ions bind to their exterior.

Discussion

Comparison of Vanadate Interactions with Phosphoenzyme-Forming Transport ATPases. There are remarkable similarities between the results reported here for vanadate binding to the H,K-ATPase and those that have been reported for vanadate binding to the Na,K-ATPase. The affinity of both enzymes for vanadate is increased by Mg^{2+}, and it is further increased by K^+. In the presence of Mg^{2+} and K^+, both enzymes bind vanadate with two affinities. At room temperature, the dissociation constants from the gastric enzyme are 5 nM and 0.5 μM, while from the Na,K-enzyme they are 4.2 nM and 0.56 μM (Cantley et al., 1978a). Vanadate interacts slowly with both enzymes. The half-time for dissociation of vanadate from the H,K-ATPase is 4.6 min, compared with the value of 3.5 min that was measured for vanadate dissociation from the Na,K-ATPase (Cantley et al., 1978a). Vanadate has been shown to inhibit the Na,K-enzyme from the cytosol (Cantley et al., 1978b). The H,K-ATPase also appears to bind vanadate from the cytosolic side, because vanadate inhibits catalysis and transport by intact gastric vesicles which are oriented inside out (Saccomani et al., 1977). Finally, both enzymes bind high-affinity vanadate and are phosphorylated with the same stoichiometry. The H,K-ATPase forms 1.5 nmol mg^{-1} phosphoenzyme and binds 1.5 nmol mg^{-1} vanadate with high affinity. The Na,K-ATPase binds one vanadate ion with high affinity per ouabain molecule bound (Cantley et al., 1978a), and there is one ouabain site per phosphorylation site (Peters et al., 1981).

In contrast to the binding results, the kinetic results obtained with the H,K-ATPase are fundamentally different from those found in kinetic studies of the Na,K-ATPase. The most important difference is that vanadate inhibited the Na,K-ATPase with a single affinity, while two inhibition constants are needed to explain the titration of H,K-ATPase activity by vanadate. Essentially all the K^+-stimulated ATPase activity of the Na,K-enzyme was inhibited by high-affinity vanadate (Cantley et al., 1978a). To explain the complex dependence of the hydrolytic rate on substrate concentration, it was proposed that the affinity of a single nucleotide site for ATP changes, along with the enzyme conformation, during the catalytic cycle (Smith et al., 1980). Vanadate inhibition of the Ca-ATPase could also be explained by a one nucleotide site two-state model, since only phosphorylation of the low-ATP-affinity Mg^{2+} conformer of the enzyme by inorganic phosphate was inhibited (Pick, 1982). In the case of the gastric H,K-ATPase, at 37 °C approximately half of both the K^+-stimulated (Figure 8) and basal Mg^{2+}-ATPase (Figure 3) activity was inhibited by high-affinity vanadate, and the other half was inhibited by vanadate with a lower apparent affinity. Biphasic inhibition cannot be easily reconciled with rapidly interconverting states of a single nucleotide site, because preferential binding of vanadate to the high-affinity state would be expected to shift the equilibrium between the states and result in inhibition of all the ATPase activity with a single apparent vanadate affinity.

Competitive Binding to Two Nucleotide Sites. The simplest explanation of biphasic inhibition is that substrate and inhibitor bind competitively to two sites. Two nucleotide sites are suggested by the complex dependence of the catalytic rate upon substrate concentration that has been observed for the gastric H,K-ATPase in several laboratories (Wallmark et al., 1980; Sachs et al., 1980; Schrijen, 1981). Evidence from direct binding measurements for two vanadate binding sites is presented in Figures 5 and 7A. The solid line in Figure 5 was calculated for dissociation constants of 5 nM and 0.5 μM that differ by 2 orders of magnitude. Dissociation constants of 20 nM and 0.6 μM, differing by more than an order of magnitude, were inferred from the Scatchard plot of the 37 °C data in Figure 7A and used to calculate the theoretical curve in the inset.

In contrast, vanadate binding to gastric vesicles in the presence of nucleotide occurred over a narrower range of free vanadate concentrations, and the titrations in Figures 6 and 7B could be interpreted as evidence for a single class of sites. Two vanadate affinities for this single site in the absence of nucleotide could be rationalized, for example, by arguing that an equilibrium between two states of the enzyme is shifted by substrate binding. However, then it would be hard to explain why two Michaelis constants are needed to describe the substrate concentration dependence of the catalytic rate, or why the stoiochimetry of acid-stabile phosphoenzyme formation

is only half the saturable vanadate binding stoichiometry. A simpler interpretation of the data in Figures 6 and 7B is that vanadate binding to two sites is poorly resolved in the presence of nucleotide because of competition between the ligands. In Table II, the substrate constants predicted from the vanadate dissociation constants used to fit the data in Figures 5 and 7A and the apparent vanadate dissociation constants shown to be compatible with the titrations in Figures 6 and 7B are compared with the Michaelis constants for high-affinity and low-affinity substrate binding that have been inferred from kinetic studies. In the calculation of the predicted values, it was assumed that vanadate and nucleotide bind competitively to two sites and that the same site has the higher affinity for vanadate both in the absence and in the presence of nucleotide. The agreement found at 37 °C, where the predicted constants fall between the reported values, no more proves that vanadate and ATP bind competitively to two sites than the roughly order of magnitude discrepancy betwen the predicted and literature values at 22 °C makes this hypothesis untenable. One objective measure of the variation that can be expected in a single constant is the 2.3–4.4-fold difference in the Michaelis constants reported at 37° C by different laboratories, so the numerical agreement between the predicted and reported values in Table II is acceptable for a comparison of two constants. Some of the differences in experimental conditions, problems in evaluating the constants, and potential artifacts in the measurements that qualify a comparison of the binding and published kinetic data are given in the footnotes to Table II. The conclusion that the vanadate binding data are compatible with competitive binding to the two kinetically defined ATP sites is strengthened by the stoichiometries that were found. These are discussed in more detail later. Here it is enough to note that the stoichiometry of 1.5 nmol mg^{-1} found for high-affinity vanadate binding corresponds to the amount of phosphoenzyme formed when only enough ATP is present to fill the high-affinity nucleotide site and that 3 nmol mg^{-1} vanadate binds both in the presence and in the absence of nucleotide.

Inhibition at Two Nucleotide Sites. The kinetic studies of vanadate inhibition reported here are also compatible with competitive binding to the kinetically defined nucleotide sites, if the slow rate of vanadate dissociation from the high-affinity vanadate site is taken into account. Competitive binding can explain biphasic inhibition of Mg^{2+}-ATPase activity, even though vanadate binds to the Mg^{2+}-enzyme with a single affinity, because ATP reacts with two Michaelis constants (Wallmark et al., 1980). Apparent inhibition constants differing by more than 2 orders of magnitude are predicted by substituting the measured vanadate dissociation constant of 0.6 μM for K_I, the ATP concentration of 2 mM for $[S]_0$, and the published K_m values of 0.4 and 50 μM into the expression for K_I(app)

$$K_I(\text{app}) = K_I(1 + [S]_0/K_m) \quad (8)$$

that assumes competitive inhibition. Conversely, the value of the Michaelis constant predicted by substituting the measured apparent vanadate dissociation constant of 13 μM for K_I(app) in eq 8 is 97 μM, which is in reasonable numerical agreement with the published K_m value for the lower affinity ATP site of 50 μM.

In contrast to ATP hydrolysis, catalysis of pNPP hydrolysis by the K^+-enzyme shows a simple dependence on substrate concentration (Forte et al., 1981). Consistent with the inference that pNPP is hydrolyzed at a single site, vanadate inhibition of pNPPase activity is monophasic (Figure 9), and the apparent vanadate dissociation constant of 130 nM found experimentally agrees well with the value of 103 nM predicted for competition between vanadate and pNPP at the high-affinity vanadate site by substituting into eq 8 the pNPP concentration of 6 mM for $[S]_0$, the measured dissociation constant from the high-affinity site of 20 nM for K_I, and the published K_m of 1.44 mM. Therefore, the dissociation half-time of 4.6 min measured by perturbing the steady-state rate of pNPP hydrolysis with vanadate is presumably the half-time for dissociation of vanadate from the high-affinity vanadate site on the K^+-enzyme.

The apparent vanadate binding constant that describes inhibition of the last 40% of the K^+-ATPase activity in Figure 8 is 3 μM. It is in good numerical agreement with the larger apparent constant of 2 μM that was estimated for dissociation of vanadate from the K^+-enzyme in the presence of nucleotide and shown in Table II to be consistent with competitive binding of the ligands to a low-affinity site. On the other hand, the first part of the kinetic titration curve in Figure 8 does not appear to be compatible with competitive binding of vanadate and ATP. The first 60% of the K^+-ATPase activity was inhibited with a vanadate binding constant of 12 nM, which is experimentally equal to the measured dissociation constant from the high-affinity vanadate site of 20 nM. One possibility is that vanadate ions and ATP bind with high affinity to physically distinct sites. This explanation of noncompetitive inhibition by high-affinity vanadate is unlikely, because nucleotide clearly did reduce the higher affinity for vanadate in the binding experiments (Figures 5–7). An alternative possibility is that ATP was unable to equilibrate with vanadate bound to the high-affinity site on the time scale of the kinetic assay. In the kinetic measurements, the enzyme was preincubated with vanadate before the reaction was started with ATP. The reaction was stopped after 15 min, which is comparable to the measured half-time of 5 min for vanadate dissociation from the high-affinity site, so it is reasonable that vanadate prebound at the high-affinity site acted like an irreversible inhibitor.

Kinetic rather than thermodynamic control was also observed in other experiments in which the enzyme was preincubated with vanadate. For example, the same apparent inhibition constant was found for phosphorylation by 2 and 200 μM ATP (Figure 4). In this case, the reaction was quenched after only 15 s, compared with the several minutes required for vanadate interaction with the Mg^{2+}-enzyme (Figure 1). The different results obtained at the same final vanadate concentration in the proton-transport experiments, depending upon the amount of vanadate with which the vesicles were preincubated (Table III), can also be explained simply by the slow rate of vanadate interaction with gastric microsomes. Had equilibrium been reached in the minute or so required to measure transport, either greater inhibition would have been observed in the constant concentration experiments or less inhibition in the constant vanadate to protein ratio experiments.

Stoichiometry of Vanadate Inhibition. The compatibility of the real and apparent dissociation constants for vanadate and ATP derived from binding and kinetic measurements with competitive binding to two nucleotide sites implies that binding 1.5 nmol mg^{-1} vanadate should half inhibit the H,K-ATPase and 3 nmol mg^{-1} bound vanadate would completely inhibit the enzyme. These predictions can be checked by comparing the binding data in Figure 7 with the kinetic data in Figure 8, which were determined under the same experimental conditions except for protein concentration. When 2.4 nmol mg^{-1} vanadate was bound to the K^+-enzyme in the presence of nucleotide, 8.6 μM vanadate remained free (Figure 7B).

Substituting these values for b and [V], and the protein concentration of 10 μg mL^{-1} used in the kinetic measurements for $[P]_0$, into the expression for the total vanadate concentration

$$[V]_0 = [V] + b[P]_0 10^{-6} \quad (9)$$

gives a pV_0 value of 5.1 which corresponds to 10.5 ± 1.5% residual K^+-ATPase activity. Since inhibition of the first 60% of the K^+-ATPase activity was apparently noncompetitive, the first titration in Figure 8 must be compared with the binding data in Figure 7A. In the absence of ATP, 0.14 μM vanadate remained free when 1.4 nmol mg^{-1} vanadate was bound, which corresponds to a pV_0 value of 6.8 and 56.5 ± 3.0% inhibition of K^+-ATPase activity. Therefore, 3 nmol mg^{-1} vanadate must bind for complete inhibition, and the break in the titration curve of K^+-ATPase activity does correlate with approximately 1.5 nmol mg^{-1} vanadate bound.

The stoichiometry of 1.5 nmol mg^{-1} found for half-inhibition of ATPase activity at 37 °C is the same as the maximum level of phosphoenzyme formation (Table I). Only the high-affinity ATP site had to be filled to give maximal phosphorylation, consistent with the observations that 1.5 nmol mg^{-1} vanadate binds with high affinity and competes with high-affinity nucleotide binding. The important implication mechanistically is that the additional activity observed at high ATP concentrations, and inhibited by 1.5 nmol mg^{-1} vanadate with low affinity, does not involve an acid-stable phosphoenzyme intermediate. The low-affinity ATP site is not simply an effector site, because the enzyme continues to turn over when the high-affinity, phosphorylatable site is completely inhibited.

A site stoichiometry of 1.5 nmol mg^{-1} implies a molecular weight of 4.7×10^5, if correction is made for 42% overestimation of the protein in gastric microsomal vesicles by the Lowry method (Peters et al., 1982). This value is an upper limit, because any inactive protein in the preparation would lead to an overestimation of the amount of enzyme. The molecular weights that have been found experimentally by radiation inactivation for the H,K-ATPase are 3.0×10^5 (Saccomani et al., 1981) and 4.44×10^5 (Peters et al., 1982).

Summary. The simplest interpretation of the data reported here for inhibition of the gastric H,K-ATPase by vanadate and vanadate binding to the enzyme is that the inhibitor binds competitively with substrate to two catalytic sites. The strongest independent evidence that there may be two nucleotide sites on the H,K-ATPase is biphasic displacement of the fluorescent ATP analogue TNP-ATP (Hiratsuka & Uchida, 1973) from the Mg^{2+}-enzyme by ADP, by β,γ-methylene-ATP, by ATP, and by vanadate ions (Sartor et al., 1982). The evidence presented that 3 nmol mg^{-1} vanadate must bind to completely inhibit ATPase activity, even though a maximum of 1.5 nmol mg^{-1} acid-stable phosphoenzyme is formed, may mean that the gastric H,K-ATPase can catalyze ATP hydrolysis via two alternative pathways. Since a different model has resulted from this study of vanadate interactions with the H,K-ATPase than was proposed for the Na,K-ATPase on the basis of studies using the same probe, it is important to point out that some more recent studies of the Na,K-enzyme using other site-specific reagents indicate that the Na,K-ATPase may contain two different nucleotide sites (Skou & Esmann, 1981; Schuurmans Stekhoven et al., 1981; Koepsell et al., 1982).

Acknowledgments

We are grateful to Herbert Cheung for fitting the relaxation curves with a nonlinear least-squares program and for helpful discussions.

Registry No. ATPase, 9000-83-3; ATP, 56-65-5; vanadate, 14333-18-7.

References

Cantley, L. C., Jr., Josephson, L., Warner, R., Yanagisawa, M., Lechene, C., & Guidotti, G. (1977) *J. Biol. Chem. 252*, 7421–7423.

Cantley, L. C., Jr., Cantley, L. G., & Josephson, L. (1978a) *J. Biol. Chem. 253*, 7361–7368.

Cantley, L. C., Jr., Resh, M. D., & Guidotti, G. (1978b) *Nature (London) 272*, 552–554.

Chang, H., Saccomani, G., Rabon, E., Schackmann, R., & Sachs, G. (1979) *Biochim. Biophys. Acta 464*, 313–327.

Cotton, E. A., & Wilkinson, G. (1974) *Anorganische Chemie*, pp 871–883, Verlag Chemie, Weinheim, West Germany.

Dean, G. A., & Herringshaw, J. F. (1963) *Talanta 10*, 793–799.

Faller, L. D., Malinowska, D. H., Rabon, E., Smolka, A., & Sachs, G. (1981) in *Membrane Biophysics: Structure and Function in Epithelia* (Dinno, M. A., & Callahan, H. B., Eds.) pp 153–174, Alan R. Liss, Inc., New York.

Forte, J. G., Poulter, J. L., Dykstra, R., Ribas, J., & Lee, H. C. (1981) *Biochim. Biophys. Acta 644*, 257–265.

Hiratsuka, T., & Uchida, K. (1973) *Biochim. Biophys. Acta 320*, 635–647.

Howlett, G. J., Yeh, E., & Schachman, H. K. (1978) *Arch. Biochem. Biophys. 190*, 809–819.

Jorgensen, P. L. (1975) *Biochim. Biophys. Acta 401*, 399–415.

Karlish, S. J. D., Beaugé, L. A., & Glynn, I. M. (1979) *Nature (London) 282*, 333–335.

Koepsell, H., Hulla, F. W., & Fritzsch, G. (1982) *J. Biol. Chem. 257*, 10733–10741.

Lopez, V., Stevens, T., & Lindquist, R. N. (1976) *Arch. Biochem. Biophys. 175*, 31–38.

Lowry, O. H., Rosenbrough, N. J., Farr, A. L., & Randall, R. J. (1951) *J. Biol. Chem. 193*, 265–275.

Macara, I. G., Kustin, K., & Cantley, L. C., Jr. (1980) *Biochim. Biophys. Acta 629*, 95–106.

O'Neal, S. G., Rhoads, D. B., & Racker, E. (1979) *Biochem. Biophys. Res. Commun. 89*, 845–850.

Peters, W. H. M., Swarts, H. G. P., de Pont, J. J. H. H. M., Schuurmans Stekhoven, F. M. A. H., & Bonting, S. L. (1981) *Nature (London) 290*, 338–339.

Peters, W. H. M., Fleuren-Jacobs, A. M. M., Schrijen, J. J., de Pont, J. J. H. H. M., & Bonting, S. I. (1982) *Biochim. Biophys. Acta 690*, 251–260.

Pick, U. (1982) *J. Biol. Chem. 257*, 6111–6119.

Pick, U., & Karlish, S. J. D. (1982) *J. Biol. Chem. 257*, 6120–6126.

Post, R. L., & Sen, A. K. (1967) *Methods Enzymol. 10*, 773–776.

Post, R. L., Park, H., & Beth, A. H. (1979) in *2nd International Conference on the Properties and Function of Na,K-ATPase* (Skou, J. C., & Norby, J. G., Eds.) pp 389–401, Academic Press, London.

Rabon, E., Chang, H., & Sachs, G. (1978) *Biochemistry 17*, 3345–3353.

Saccomani, G., Stewart, H. B., Shaw, D., Lewin, M., & Sachs, G. (1977) *Biochim. Biophys. Acta 465*, 311–330.

Saccomani, G., Crago, S., Helander, H. F., Dailey, D. W., Chang, H. H., & Sachs, G. (1979) *J. Cell Biol. 83*, 271–283.

Saccomani, G., Sachs, G., Cuppoletti, J., & Jung, C. Y. (1981) *J. Biol. Chem. 256*, 7727–7729.

Sachs, G., Berglindh, T., Rabon, E., Stewart, H. B., Barcellona, M. L., Wallmark, B., & Saccomani, G. (1980) *Ann.*

N.Y. Acad. Sci. 341, 312–334.
Sartor, G., Mukidjam, E., Faller, L., Saccomani, G., & Sachs, G. (1982) Biophys. J. 37, 375a.
Schrijen, J. I. (1981) Ph.D. Dissertation, University of Nijmegen, The Netherlands.
Schuurmans Stekhoven, F., & Bonting, S. L. (1981) Physiol. Rev. 61, 1–76.
Schuurmans Stekoven, F. M. A. H., Swarts, H. G. P., de Pont, J. J. H. H. M., & Bonting, S. L. (1981) Biochim. Biophys. Acta 649, 533–540.
Skou, J. C., & Esmann, M. (1981) Biochim. Biophys. Acta 647, 232–240.
Smith, R. L., Zinn, K., & Cantley, L. C. (1980) J. Biol. Chem. 255, 9852–9859.
Uspensky, J. V. (1948) Theory of Equations, pp 82–98, McGraw-Hill, New York.
Van Etten, R. L., Waymack, P. P., & Rehkop, D. M. (1975) J. Am. Chem. Soc. 96, 6782–6785.
Wallmark, B., & Mardh, S. (1979) J. Biol. Chem. 254, 11899–11902.
Wallmark, B., Stewart, H. B., Rabon, E., Saccomani, G., & Sachs, G. (1980) J. Biol. Chem. 255, 5313–5319.
Yoda, A., & Hokin, L. E. (1980) Biochem. Biophys. Res. Commun. 40, 880–884.

Specific Photoaffinity Labeling of the Digitalis Binding Site of the Sodium and Potassium Ion Activated Adenosinetriphosphatase Induced by Energy Transfer†

Maurice P. Goeldner,* Christian G. Hirth,* Bernard Rossi,‡ Gilles Ponzio,‡ and Michel Lazdunski‡

ABSTRACT: A ouabain *p*-aminobenzenediazonium derivative with a high specific radioactivity has been synthesized from ouabain and used as a photolabel for the (sodium plus potassium)-activated adenosinetriphosphatase from *Electrophorus electricus* electric organ and from dog kidney. In the dark it binds reversibly to the digitalis receptor site, with binding characteristics comparable to those of ouabain. The photoactivation of the ouabain derivative to produce covalent labeling of the receptor was obtained by energy transfer from a tryptophan residue in the (Na^+,K^+)ATPase to the ouabain *p*-aminobenzenediazonium molecule bound at the active site. The great advantage of this procedure compared to previous methods is that free molecules of the photoactivatable derivative are not photodecomposed. Analysis of the photolabeled polypeptides on sodium dodecyl sulfate gel electrophoresis showed that over 90% of the total radioactivity incorporated was found in the large molecular weight α-chain of the kidney enzyme (M_r 93 000). The same specific labeling of the α-subunit was obtained with a crude microsomal fraction from *Electrophorus electricus*. A mild tryptic fragmentation of the subunit into two peptide fragments of M_r 58 000 and 41 000, respectively, shows that the digitalis receptor is located in the N-terminal 41 000 fragment.

The (Na^+,K^+)ATPase[1] catalyzes the cotransport of Na^+ and K^+ through the plasma membrane. The enzyme is composed of an α-chain (M_r 90 000–100 000) which is known as the catalytic subunit and of a glycosylated β-chain (M_r 45 000–58 000) which has no known function. The presence of a smaller γ-subunit which is a proteolipid component has also been described [for references see Jørgensen (1982)].

Digitalis compounds like ouabain specifically inhibit cell functions carried out by the enzyme, i.e., Na^+ and K^+ transport and ATP hydrolysis. These molecules interact with a site situated on the extracellular surface of the (Na^+,K^+)ATPase molecule. The ouabain binding site has two functionally distinct regions, one specific for the lactone ring and the steroid portion and one specific for the sugar moiety. Digitalis compounds are particularly important in heart pharmacology since they are among the most potent cardiotonic drugs. For all these reasons extensive efforts have been made to know more about the digitalis binding sites [for references see Jørgensen (1982)].

A general procedure for making compounds which provoke photosuicide inactivation of enzymes and receptors has been described recently. The procedure consists in using an aryldiazonium derivative as a photoactivatable label (Goeldner & Hirth, 1980; Goeldner et al., 1982) which produces its photodecomposition after it is complexed through the receptor site. The photodecomposition is induced by energy transfer through a tryptophan residue of the receptor.

The present paper describes the synthesis and the properties as an affinity label for the (Na^+,K^+)ATPase of ouabain *p*-aminobenzenediazonium derivative (ABD-ouabain), an ouabain derivative producing a photosuicide inactivation of the enzyme.

Experimental Procedures

Materials

Ouabain, diphenylcarbamoyl chloride (DPCC) treated trypsin, and the diTris salt of *p*-nitrophenyl phosphate were obtained from Sigma. [^{3}H]Ouabain (14 Ci/mmol) was ob-

† From the CNRS, Centre de Neurochimie, 67084 Strasbourg Cedex, France. *Received January 20, 1983.* This work was supported by the Centre National de la Recherche Scientifique, the Délégation Générale à la Recherche Scientifique et Technique (Grant 81.E.1204), the Institut National de la Santé et de la Recherche Médicale (Grant 131006), and the Fondation de la Recherche Médicale.

‡ Present address: Centre de Biochimie du CNRS, Faculté des Sciences, Parc Valrose, 06034 Nice Cedex, France.

[1] Abbreviations: ABD-ouabain, ouabain *p*-aminobenzenediazonium derivative; APh-ouabain, ouabain *p*-aminophenol derivative; DDF, *p*-(dimethylamino)benzenediazonium fluoroborate; Boc, *tert*-butyloxycarbonyl; THF, tetrahydrofuran; TFA, trifluoroacetic acid; TEA, triethanolamine; DPCC, diphenylcarbamoyl chloride; NMR, nuclear magnetic resonance; MS, mass spectrometry; (Na^+,K^+)ATPase, (sodium plus potassium)-activated adenosinetriphosphatase; EDTA, ethylenediaminetetraacetic acid; SDS, sodium dodecyl sulfate.

0006-2960/83/0422-4685$01.50/0